Interaction of hydrogen with the Ag(110) surface

P. T. Sprunger*
Department of Physics, University of Pennsylvania, Philadelphia, Pennsylvania 19104-6396

E. W. Plummer
Department of Physics, University of Tennessee, Knoxville, Tennessee 37996-1200
and Solid State Division, Oak Ridge National Laboratory, Oak Ridge, Tennessee 37831-6057
(Received 11 January 1993; revised manuscript received 29 July 1993)

The interaction of atomic and molecular hydrogen with the (110) surface of silver has been studied using electron-energy-loss spectroscopy, thermal desorption spectroscopy, low-energy electron diffraction (LEED), and work-function measurements. No evidence for associative or dissociative chemisorption of H_2 is observed at the substrate temperatures investigated (≥ 90 K). However, at 100 K, atomic hydrogen bonds in the $[1\,\bar{1}\,0]$ troughs of the surface in tilted-trigonal sites. As a function of concentration, a sequence of lattice-gas superstructures is observed with LEED including (1×4), (1×3), (2×6), and (2×2) patterns. At saturation coverage, the work function increases by 0.22 eV. However, this phase is metastable; upon annealing, hydrogen desorption is accompanied by an irreversible transition to a new bonding geometry in which LEED shows a dim (1×2) superstructure. The desorption of molecular hydrogen is characterized by two overlapping peaks centered at ~ 155 K [6.9 kJ/mol] and ~ 180 K [9.9 kJ/mol] which obey first- and second-order kinetics, respectively. Various structural models and hydrogen site assignments are discussed in comparison with data for similar systems.

I. INTRODUCTION

The interaction between hydrogen and clean metal surfaces has been the focus of numerous experimental and theoretical investigations.[1] Motivated by both its technological importance and its theoretical attractiveness, studies have sought to identify and explain the induced structural, electronic, and chemical perturbations which accompany hydrogen physisorption and chemisorption on well-characterized metal substrates. Theoretically, the hydrogen atom may appear to be the simplest adsorbate (a single interacting electron), however, experimentally its interaction with metal surfaces has been shown to be quite complex due to its small atomic size and relatively strong bond. This complexity includes hydrogen absorption into subsurface/bulk sites, surface quantum delocalized motion, formation of surface/bulk hydrides, and substrate structural reconstructions/relaxations.

These effects are especially prevalent in the case of hydrogen interaction with substrates with "open" crystal faces, such as the fcc(110).[2] Some fcc(110) surfaces have an inherent instability, for example, the clean $5d$ metals (Pt, Ir, and Au) undergo (1×2) missing-row reconstructions.[3–6] Moreover, a calculation of the relative stability of the clean (1×1) compared to a missing-row (1×2) structure of Ag(110) indicates the existence of a very small difference between the corresponding surface energies ($\cong 2.3$ meV/Å^2). This indicates that there is a near instability of this clean surface towards strong reconstruction (large mass transport).[7] Furthermore, depending on local surface-subsurface concentration and substrate temperature, adsorption of hydrogen is known to induce various structural changes on other metal surfaces with twofold symmetry [fcc(110) and hcp(100)] including Ni, Cu, Rh, and Pd(110).[1–2] The amount of hydrogen-induced substrate displacement on these surfaces ranges from a small normal rippling of substrate $[1\bar{1}0]$ atomic rows (see Fig. 2—parallel to first-layer rows), to an in-plane row-pairing (lateral movement), to a large mass transport creating a 1×2 missing-row-type reconstruction. Using He diffraction, Cantini *et al.* have identified an induced surface "rippling" of one specific phase of the D/Ag(110) system.[8]

While a large number of investigations focuses on surface structural changes, energetics, and kinetics of many H/fcc(110) systems, very little is known concerning the H/Ag(110) system.[8,9] This is in part a consequence of the small probability of dissociative chemisorption of molecular hydrogen on this and other noble- and simple-metal surfaces. In these systems, dissociative adsorption is an activated process.[10] Because of the differences in electronic structure (filled d bands), one expectation is that the H/Ag system should be more similar to other H/noble-metal systems than to that of H/transition-metal systems. Effective-medium-based calculations predict a weakening of the H chemisorption energy as a given d band is filled and thus the binding energy on noble metals is less than the corresponding transition metals; however, the energy gained due to the hybridization of the hydrogen state with the unfilled d states is a relatively small component of the total chemisorption energy.[11] Thus, the H/Ag system should be similar to other noble-metal systems with respect to the activated adsorption; but once adsorbed, chemisorption properties could be quite similar to transition-metal surfaces. Based on our results of low-energy electron diffraction (LEED), high-resolution electron-energy-loss spectroscopy (HREELS), thermal desorption spectroscopy (TDS), and

0163-1829/93/48(19)/14436(11)/$06.00

$\Delta\Phi$ spectroscopy, we have found that this is essentially correct; the H/Ag(110) system indeed bears close similarities to both transition-metal and other noble-metal systems.

In this paper, we report experimental data and suggest hydrogen bonding sites and adsorbate structural models as a function of both coverage and substrate temperature. It is found that on Ag(110) the following occurs. (1) H_2 is neither dissociatively nor associatively chemisorbed over the temperature range studied; however, atomic hydrogen is chemisorbed at 100 K. (ii) At this temperature, hydrogen occupies a single binding site for all coverages. Because of strong adsorbate interaction, hydrogen forms various lattice-gas superstructures as a function of coverage. These lattice-gas phases are accompanied by small atomic displacements of the substrate (weak reconstruction). (iii) Upon thermal annealing to ~ 165 K, H_2 desorption is accompanied by a restructuring of the surface in which hydrogen occupies a new bonding geometry; thus, the low-temperature phase is energetically metastable. (iv) The desorption of molecular hydrogen is characterized by two overlapping peaks centered at ~ 155 K (0.30 eV/molecule) and ~ 180 K (0.43 eV/molecule) which obey first- and second-order kinetics, respectively.

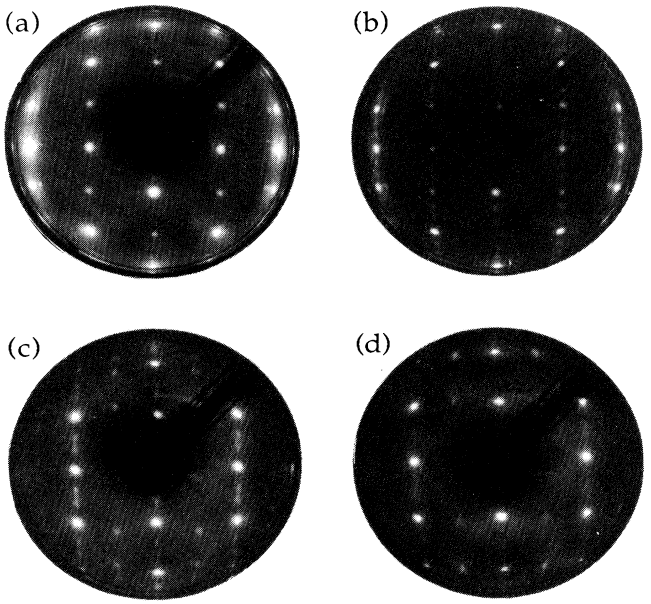

FIG. 1. The LEED pattern of (a) clean (1×1) (140 eV); (b) 0.7 L hydrogen (1×3) (140 eV); (c) 1 L hydrogen (2×6) (90 eV); and (d) 15 L hydrogen (2×3) (90 eV). Sample temperature = 100 K.

II. EXPERIMENTAL DETAILS

The Ag(110) crystal was cut to within $\pm 0.5°$ from a single-crystal rod and mechanically polished. Upon introduction into the UHV chamber (base pressure $= 5\times 10^{-11}$ Torr), the sample was cleaned by repeated cycles of sputtering with 1-keV Ne+ions (~ 30 min) at room temperature and subsequent annealing to ~ 725 K for 10 min. At the end of the cleaning cycle, the 1×1 LEED pattern was quite sharp [see Fig. 1(a)] with low background. Sample cleanliness was monitored with HREELS and Auger-electron spectroscopy. Measurement of work function changes ($\Delta\Phi$) due to exposure of hydrogen was carried out using the EELS operated in a retarding field mode[12] with an incident-beam energy of 30 eV. HREELS spectra were taken with the normal scattering plane aligned within $\sim 3°$ along $[1\bar{1}0]$ or [001] directions and had typical elastic peak resolutions of 4.5–8 meV in the specular direction (60° from normal).

Dosing of either atomic or molecular hydrogen (or deuterium) was performed with the sample held at ~ 100 K. Atomic H was produced by passing H_2, at room temperature, through a hot W doser located 1.5 cm from crystal face. Since the dissociation efficiency of the doser is not known and there is no absolute calibration of the H coverage, H doses are reported in units of dissociated-H_2 exposure (1 L $= 10^{-6}$ Torr s). Furthermore, reported coverages (Θ_H) are relative to the maximum integrated TDS spectra ($\Theta_H \equiv 1$) and thus do not refer to absolute hydrogen monolayers. The TDS temperature ramp was held at a linear rate of 1 K/s.

Intensity of diffraction spots was measured with a computer video system from the reverse viewing LEED system. Intensities of equivalent beam spots, normalized to an average background, were recorded automatically as a function of incident energy with the sample at ~ 100 K.

III. RESULTS AND INTERPRETATION

A. Molecular hydrogen

Exposing the clean Ag(110) surface (≥ 100 K) to room temperature H_2 (or D_2) resulted in no observable change in the surface as determined by HREELS, work-function measurements, TDS, or LEED. Thus, neither associative nor dissociative chemisorption of H_2 takes place for the temperature range studied due to a large activation energy barrier. This result is consistent with both theoretical predictions[13–15] and experimental results of other noble- (Cu, Ag, and Au) (Refs. 16–20) and simple-metal (Al, Be, Mg, Li, and K) (Refs. 21–24) surfaces. The majority of these investigations conclude that the height of this activation barrier is characteristically large (~ 0.5–1 eV). It is generally assumed that the lack of d holes at the Fermi level (E_F) in simple and noble metals prohibits the direct overlap of the H_2 bonding orbital ($1\sigma_g$) with the filled s-electron density of the metal (Pauli repulsion); consequently, dissociative chemisorption is an activated process. In the case of transition metals, which have empty d states at E_F, direct dissociative chemisorption of H_2 is typically nonactivated. Because of the low thermal kinetic energy associated with room temperature H_2, our results of the Ag(110) system only confirm that the activation energy is larger than kT as is shown in similar systems.

B. Atomic hydrogen structure at 100 K:LEED

The activation barrier to H_2 dissociative adsorption can be experimentally surmounted by exposing the clean surface directly to atomic hydrogen, that is, the heat of dissociation of H_2 (4.52 eV/molecule) is externally supplied. Adsorption of atomic hydrogen (deuterium) at ~ 100 K produces a continuous sequence of LEED patterns as a function of increasing coverage [Figs. 1(a)–1(d)]. At the lowest coverages, only dim streaks between the [001] integer-order spots are visible. This probably corresponds to small domain mixtures of $(1\times n)$ superstructures, where $n \geq 4$, because at slightly higher coverages clear regions of (1×4) are discernible. From H_2 TDS integration results, this structure occurs around a hydrogen coverage equal to only 20% of saturation ($\Theta_H \cong 0.20$). Because of spatial inhomogeneity of atomic hydrogen flux at this low coverage, clear (1×4) LEED patterns across large areas of the sample were not reproducible.

At exposures corresponding to approximately $\Theta_H \cong \frac{1}{3}$, fractional one-third-order spots along the [001] direction are relatively intense and homogeneous across the entire crystal surface [Fig. 1(b)]. There seems to be a propensity for the formation of this (1×3) structure, suggesting that this phase is relatively stable. From video-LEED intensity profiles, the full width at half maximum (FWHM) of the integer-order spots are 1.4°, whereas the fractional-order spots are 2.4° at an energy of 140 eV. Assuming the angular width of the integer-order spots approximates the instrumental resolution, a simple calculation[25] reveals that this (1×3) structure has a domain size of ~ 30 Å along the [001] direction and corresponds to only ~ 7 Ag(110) unit cells.

Additional hydrogen exposure in the range of $\Theta_H \cong \frac{1}{2}$ to $\Theta_H \cong \frac{3}{4}$ formed, in general, a (2×6) structure [Fig. 1(c)]. However, in this coverage region, the LEED pattern is sometimes characterized by mixtures of different structures. For example, the (1×3) "extra" spots elongate so that clear distinction between a (2×4) and (2×6) is obscured. Furthermore, the "split" half-order spots along the $[1\bar{1}0]$ direction appear to move continuously together as coverage increases. This suggests that over this exposure region, small domains of differing overlayer structures exist.

Finally, at saturation coverage ($\Theta_H \equiv 1$), the (2×6) fractional-order spots coalesce into single spots giving rise to a (2×2) LEED structure [Fig. 1(d)]. The half-order "extra" spots along the [001] direction are dim and elongated. The fact that the $(\pm\frac{1}{2},0)$ spots are missing suggests a (2×1) structure; because of a glide-line symmetry, there is an absence of $(\pm n/2,0)$, with n odd, diffraction spots in the (2×1)-2H structure. It is believed that at hydrogen saturation the "(2×2)" structure may be a mixture of two differing domains, namely, (2×1) and (1×2) ordered superstructures.

Because of the small size and atomic number, hydrogen has a small diffractive power in a LEED experiment. Consequently, "extra" diffraction spots due to scattering solely from an ordered array of protons (lattice gas) are much less intense (e.g., $\frac{1}{100}$) than typical "substrate" spots. If strong reconstruction (e.g., large substrate mass transport) accompanies the adsorption of hydrogen, "extra" spots are typically of the same intensity as the substrate; that is, they originate from the scattering of surface substrate atoms with a different symmetry. However, if the intensity of the "extra" spots is in between these two limits, there is less certainty about the origin of the observed LEED patterns.[1] At certain energies, the "extra" spots of this H/Ag(110) system were fairly strong, up to $\sim\frac{1}{3}$ as intense as the substrate spots. However, in order to quantify an energy-averaged intensity ratio, certain fractional-order (f) and integer-order (i) diffraction spot intensities, $I(E)$, were recorded as a function of incident energy using the video-LEED system. Following a definition used by Puchta *et al.*, a comparison ratio (v) between these two sets can be calculated,[26]

$$v = \sum_f \frac{1}{\Delta E_f} \int I_f(E)dE \Big/ \sum_i \frac{1}{\Delta E_i} \int I_i(E)dE \ . \qquad (1)$$

Using this method, between an energy range of 45 and 230 eV, the intensity ratio v for the (1×3) LEED structure[27] [see Fig. 1(b)] was determined to be 14%.[28]

This ratio is far from unity, suggesting that there is not a hydrogen-induced reconstruction of a strong type (e.g., missing row, row pairing). Moreover, this quantity is a magnitude larger than, for example, the H/Ni(111) (Ref. 29) system (1–2 %) whose "extra" spots are believed to be due to scattering solely from a symmetric array of hydrogen atoms. This typical ratio v for this H/Ag(110) system is in an intermediate range and is quite similar to the H/Rh(110)-(1×2) phase ($v_{Rh} \cong 10\%$) (Ref. 25) or $-(1\times 3)$ phase ($v_{Rh} \cong 5\%$).[30] From a detailed LEED-*IV* analysis, these H/Rh LEED patterns were determined to originate from a hydrogen lattice-gas superstructure accompanied by a weak substrate reconstruction. That is, this hydrogen phase induces small lateral and normal surface Rh displacements (~ 0.04 Å) from the clean (1×1) equilibrium positions. It is also believed that the observed LEED patterns for this H/Ag system are due to the formation of ordered hydrogen superstructures, or lattice-gas phases, accompanied by some degree of weak substrate reconstruction.

Very similar sequences of hydrogen lattice-gas superstructures have been observed with LEED on other systems which have twofold symmetry. It is believed that long-range repulsive H-H interactions along the [001] direction, which are mediated indirectly though the substrate, coupled with a short-range H-H interaction along the $[1\bar{1}0]$ direction dictate the exact superstructure phases.[1] Evidence of this H-H interaction is also suggested from the EELS and $\Delta\Phi$ data and is detailed below. In Figs. 2(a)–2(c), suggested lattice-gas models are shown. The proposed fundamental building block of all superstructures is the so-called "zig-zag" chain in which H atoms lie in tilted-trigonal sites (discussed below) along the $[1\bar{1}0]$ rows of the first-layer Ag atoms. Because of this long-range repulsive H-H interaction (or row-row interaction), the average distance between "zig-zag" chains decreases as H coverage increases. Thus, at low coverages, the $(1\times n)$ LEED patterns indicate an average dis-

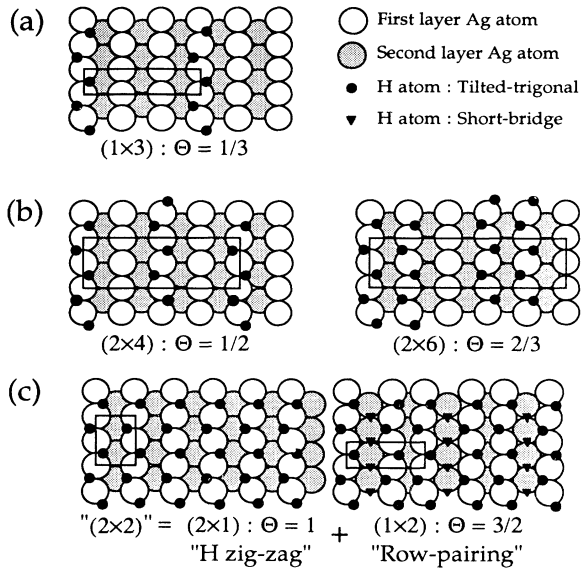

FIG. 2. Structural models of ordered low-temperature H phases: (a) "(1×3)" phase ($\Theta_H \approx \frac{1}{3}$); (b) (2×4) and (2×6) phases ($\Theta_H \approx \frac{1}{2} - \frac{2}{3}$); and (c) "(2×2)" phase at saturation coverage.

tance between chains of n unit Ag cells along the [001] direction. This is shown in Fig. 2(a) for $n = 3$. Although this structure should correspond to a (2×3) LEED pattern, it is believed that there is a random sequence, or phase, of the zig-zag chains with respect to ordering along the $[1\bar{1}0]$ direction because of the large chain-chain separation.[31] Thus, the "(1×3)" LEED pattern reflects "zig-zag" chain order along the [001] direction only. However, because there is a lack of diffuse "streaks" which reflect this proposed disorder along the $[1\bar{1}0]$ direction, it is suggested that other structural factors contribute to the observed (1×n) patterns.

In the case of H/Cu(110) (Ref. 32) and H/Rh(110) (Ref. 30), the observed (1×3) LEED patterns are attributed, in part, to a small hydrogen-induced reconstruction which involves small outward corrugation of every two or three $[1\bar{1}0]$ rows. As suggested above, it is believed that the H/Ag(110)-(1×3) structure also includes a degree of weak reconstruction, perhaps very similar to these H/Cu and Rh systems. Effective-medium-based calculations of the Cu(110) system support this concept of local H-induced distortions.[33] However, these same type of calculations also predict that between the $[1\bar{1}0]$ rows the potential is very flat. Consequently, hydrogen will be delocalized[34] and at low coverages, $\Theta_H < \frac{1}{2}$, H-H interaction is small and no long-range order is predicted. Observation of an ordered LEED pattern of the Ag(110) with as little as $\Theta_H \cong \frac{1}{4}$ lies in partial contrast to this theoretical prediction of the H/Cu(110) system; long- and short-range order is observed along the [001] direction but a lack of long-range order is observed along the $[1\bar{1}0]$ direction (random phases between adjacent H zig-zag rows).

Possible models of the (2×4)/(2×6) and "(2×2)" LEED structures are shown in Figs. 2(b) and 2(c). The (2×4)/(2×6) formations are due to the repulsive chain-chain interactions along [001] and consequent maximal separation at a given hydrogen coverage. However, the distance between adjacent "zig-zag" rows is now small enough to dictate order between the relative H phases along the $[1\bar{1}0]$ direction. There is a phase shift between neighboring zig-zag chains (or pairs of chains) with respect to the hydrogen positions. As the hydrogen coverage increases, the chain density also increases until each Ag $[1\bar{1}0]$ row is saturated by H atoms [see Fig. 2(c), left-hand side]. At $\Theta_H = 1$ for Co($10\bar{1}0$), Ni(110), and Pd(110), it is believed that these surfaces are saturated by these "zig-zag" rows forming a (2×1)-$p2mg$ LEED pattern[1] at low temperature. However, it is believed that these phases do not contain appreciable local substrate atomic displacements, that is, the "extra" LEED spots are due to hydrogen scattering only.

In the case of Ni(110) at low temperatures, the surface is not yet saturated at a coverage of $\Theta_H = 1$. Increasing the coverage to $\Theta_H = 1.5$ causes the surface to undergo a reconstruction of the strong type (row pairing) and the resulting (1×2) LEED pattern is also associated with a new EELS spectrum; the hydrogen occupies two nonequivalent tilted-trigonal sites in the row-pairing structure.[35] As already stated for the H/Ag(110) system, the "(2×2)" structure observed at saturation coverage may be a small domain mixture of these latter two H/Ni(110) phases. Tentative results of a nuclear reaction analysis (NRA) experiment indicate that the "(2×2)" LEED structure occurs at an absolute coverage of ~1.25 ML D per Ag(1×1) surface atom. This result corroborates the proposal that the surface contains small domain mixtures of (2×1)-1 H and (1×2)-1.5 H structures. However, an alternative approach is that in the highest coverage region, some amount (~0.25 ML) of hydrogen migrates into the subsurface region. Occupation of these tetrahedral and/or octahedral subsurface sites could induce local surface distortions, as has been predicted for similar systems,[33,36] giving rise to the observed (2×2) LEED pattern.

C. Atomic hydrogen bonding at 100 K:EELS and $\Delta\Phi$

The LEED data presented above reflect information about the hydrogen interaction over a somewhat large length scale; that is, formation of lattice-gas structures. HREELS data reflect very local chemisorption information. With the sample at ~100 K, a series of specular direction HREELS spectra (Fig. 3) is shown as a function of atomic hydrogen exposure through saturation coverage. Adsorption of atomic deuterium shifts these loss peaks in energy by approximately $1/\sqrt{2}$, confirming that they are attributable to H-induced losses and not to contamination. Each spectrum is dominated by two losses (~60 and 105 meV) which increase in intensity with exposure. The relatively large intensity of the losses, normalized to the elastic peak, suggests that hydrogen is adsorbed on top of the surface, that is, the dynamic dipole lies above the surface plane. For all incident electron en-

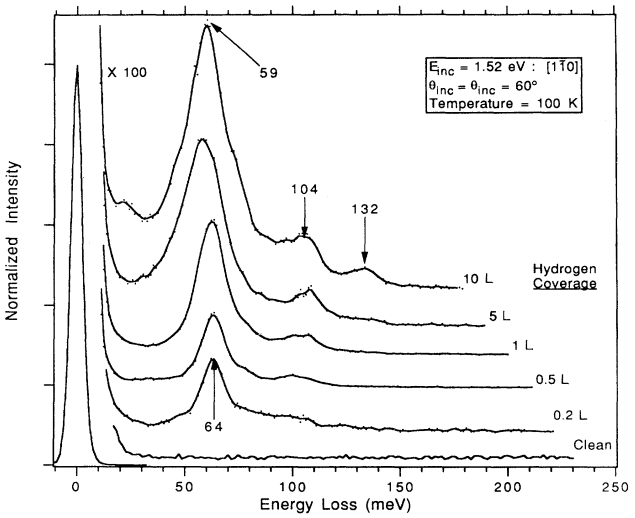

FIG. 3. Low-temperature specular EELS spectra as a function of atomic hydrogen exposure.

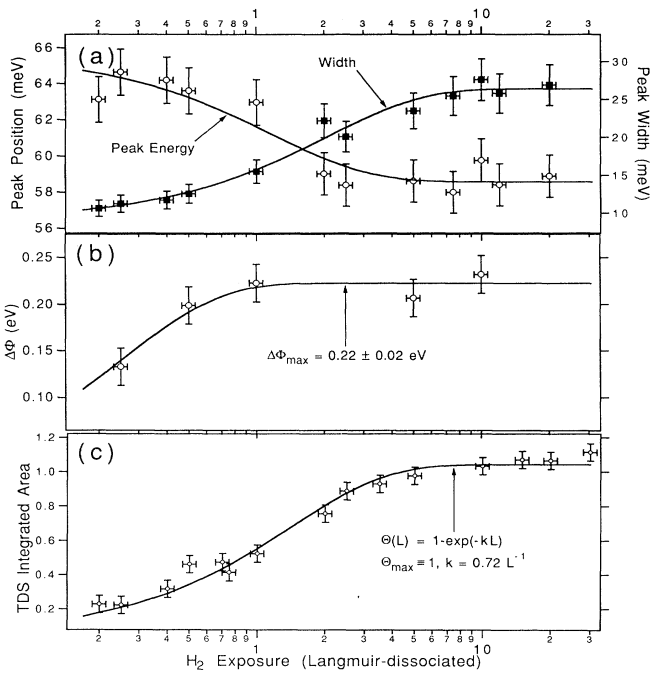

FIG. 4. As a function of atomic hydrogen coverage (a) the peak energy and width of ~60-meV EELS loss; (b) the work-function change; (c) the integrated H_2 TDS signal (with fit).

ergies investigated (1.5, 2.5, 4, 7, and 12.7 eV), the relative loss intensities remained approximately constant indicating a lack of any resonant process occurring in the scattering mechanism.[37]

The HREELS spectra suggest, especially at low coverage, that the losses are due to localized vibrational losses in contrast to delocalized "quantum motion."[29,33,38] In the latter case, surface hydrogen motion is described in terms of "protonic" two-dimensional energy bands. It has been proposed that this effect occurs in many systems including H/Cu(110).[39] This type of hydrogen phase is characterized by a decreasing loss width as concentration, or short-range H-H interaction, increases. However, the width (after deconvolution with elastic peak) of the ~60-meV loss increases with coverage [Fig. 4(a)]. Furthermore, the lack of "protonic-" type energy shifts in the HREELS data of this system indicates that hydrogen can be adequately described by localized vibrations about an equilibrium position at all coverages. As noted above, this conclusion is also corroborated by the LEED observation of well-defined superstructures at very low coverages.

The EELS spectra in Fig. 3 indicate that independent of hydrogen concentration, the intensity ratio between the ~60- and 105-meV losses remains approximately constant. This suggests that these losses can be assigned to two vibrational modes corresponding to hydrogen occupying a single bonding site on the surface. Thus, at low temperature, hydrogen predominantly occupies one bonding site throughout all coverages. Using different EELS scattering geometries, the dominant 60-meV loss is found to be dipole active, whereas the less intense peak at 105 meV has a smaller dipole-active component. Although specular loss spectra appear the same along both the [001] and [1$\bar{1}$0] scattering directions (see Fig. 5), off-specular EELS shows a distinct difference. The 105-meV loss along the [001] scattering direction follows a nearly dipolar intensity drop off; however, a strong impact scattering loss is observed at approximately this energy with the scattering plane along the [1$\bar{1}$0] direction (parallel to the rows).

Utilizing EELS selection rules[40] along with the possible high-symmetry bonding sites on a fcc(110) surface where hydrogen may be adsorbed, only one site has the required symmetry to fit the observed dominant losses in the EELS data, namely, the tilted-trigonal site. In this position, the hydrogen is located at the apex of three Ag

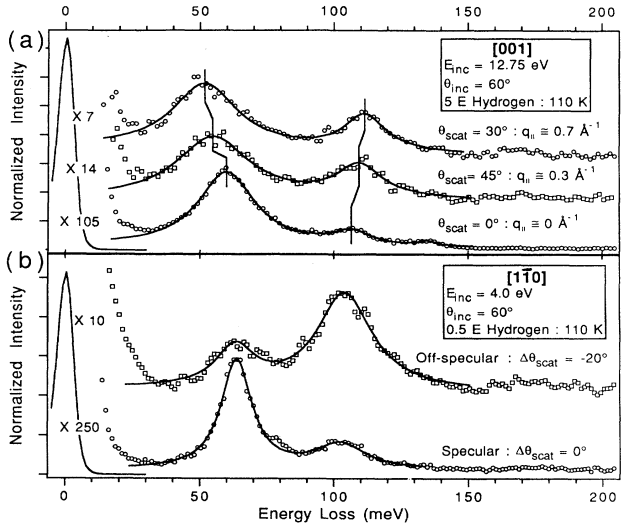

FIG. 5. Off-specular low-temperature EELS spectra: (a) scattering plane along the [001] direction and (b) scattering plane along the [1$\bar{1}$0] direction.

atoms located within the [1$\bar{1}$0] troughs. The normal vibration is along the ⟨111⟩ direction, that is, tilted ~35° with respect to the [110] surface normal. This adsorption site has C_s symmetry and should have two dipole-active modes (A':$\omega_\perp$ and $\omega_\parallel$ [001]) with scattering along the [001] direction. However, with scattering along the [1$\bar{1}$0] direction, the tilted-trigonal site has two dipole-active modes (A':$\omega_\perp$ and $\omega_\parallel$ [001]) and one nondipole active mode (A'':$\omega_\parallel$ [1$\bar{1}$0]). Although the EELS spectra in Fig. 5 do not exactly reflect these predictions, the spectra have many of the required characteristics for hydrogen bonding in the tilted-trigonal site. Of the possible hydrogen bonding sites, only one has the requisite of having two distinct dipole-active losses as is seen in our EELS data. From symmetry arguments, there should be a third mode (A'') observed in the off-specular EELS spectrum along the [1$\bar{1}$0] direction. In this geometry, the increase in intensity around ~105 meV [see Fig. 5(b)] may be due to this third mode since there is a lack of similar enhancement with scattering along the [001] direction. That is, if the energy of the A'' mode was almost degenerate with one of the A' modes (~105 meV) the general features of the specular and off-specular EELS spectra would be reproduced.

The assignment of the tilted-trigonal site as the equilibrium bonding position is supported by a comparison to the results of similar systems. Experimental studies of other H/fcc(110) systems, including Ni (Refs. 35 and 41), Rh (Refs. 26 and 42), Co (Ref. 2), and Pd (Refs. 43 and 44), conclude that hydrogen bonds preferentially in tilted-trigonal sites at low temperatures and also undergoes very similar lattice-gas structural sequences as observed with LEED. For the H/Cu(110) system, which should arguably be similar to the Ag(110) system, a recent EELS study concludes that the corresponding equilibrium position is also the tilted-trigonal site[39]; however, two other EELS studies have assigned the hydrogen to occupation of long-bridge and/or fourfold-coordinated sites.[32,45]

It is believed that the ~58-meV loss (A' mode) corresponds to the H motion which is perpendicular to the ⟨111⟩ direction and along the [001] direction, that is, the $\omega_\parallel$ [001] vibration. The "normal" mode (A':$\omega_\perp$) is then assigned to the ~104-meV loss and has a smaller EELS intensity than the ~58-meV loss. Although the "normal" vibration of a H/metal system typically produces the largest intensity in an EELS spectrum, H-site bonding geometry (threefold site canted with respect to the surface normal) of this system produces a unique screening of the H-Ag dipolar vibrations. This loss assignment is based on many factors. An analysis of the H/Ag(111) system shows that adsorption at 100 K produces one loss in EELS spectra. This dipole-active mode has been tentatively assigned to the normal vibration ($\omega_\perp$) of hydrogen occupying threefold hollows,[46] a site which is common on surfaces with C_{3v} symmetry. As seen in Figs. 6(b) and 6(c), the energy of the H/Ag(111) vibrational loss is almost equivalent to the "normal" mode (A':$\omega_\perp$) of H/Ag(110), that is ~104 meV. This is not surprising, since the geometry of the sites is locally equivalent and thus is expected to have nearly equivalent loss energies.

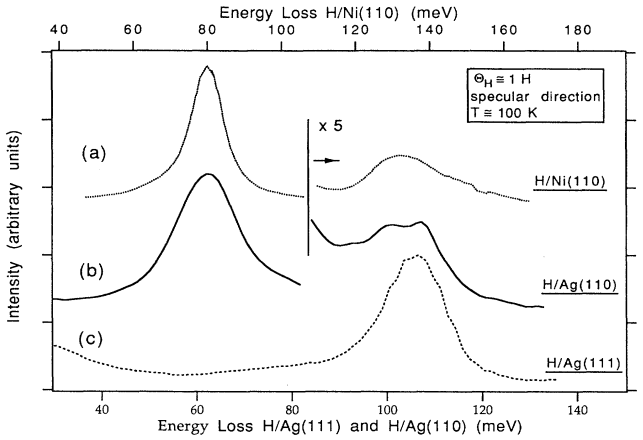

FIG. 6. Comparison of low-temperature EELS spectra of hydrogen vibrational losses of three different systems: (a) Ni(110)-(2×1) H (from Ref. 35); (b) Ag(110) ~(2×6) phase; (c) Ag(111) is approximately saturated coverage. (Note the different energy axes for Ni and Ag.)

Furthermore, except for an energy scaling (x1.28), the H/Ag(110) EELS spectrum is almost identical to that of the H/Ni(110)-(2×1) system [see Figs. 6(a) and 6(b)], wherein a similar mode assignment was concluded. Although this comparison is not unequivocal, the striking similarity between the two EELS spectra implies that the hydrogen bonding of these two systems is similar, and thus supports the mode assignments of the H/Ag(110) system.

As is seen in Fig. 3, the ~60- and ~105-meV losses dominate the EELS spectra; however, there is an additional weak loss at ~130-meV which only occurs at the highest hydrogen coverages. The relatively high energy of this mode suggests that this loss is due to occupation of lower coordination sites, such as a short-bridge site. As in the case of the H/Ni(110) system at saturation coverage,[35] the ~130-meV mode of this system may originate from occupation of new bonding sites associated with a row-pairing reconstruction, possibly the short-bridge site within the [1$\bar{1}$0] troughs. As already stated, the H saturated "(2×2)" LEED pattern may be due to mixtures of (1×2) and (2×1) superstructures [see Fig. 2(c)], which could arise from row-pairing and zig-zag structures, respectively.

The EELS spectra show that as a function of coverage, the vibrational losses shift in energy and width. The peak position of the dominant loss shifts [Fig. 4(a)] from 64 meV at low coverages to 58 meV at hydrogen saturation as determined by fitting each spectrum with a sum of two loss functions. Although obviously due to changes in the potential-energy surface (PES) and the accompanying changes in the bonding geometry, the exact mechanism for this change is not known. As surface concentration increases, lateral H-H interactions (direct or indirect) lead to changes in the PES and subsequently affect vibrational modes. Analogous to observations of the H/Cu(110) (Ref. 45) system, the large surface interlayer contraction ($\Delta d_{12} = -9\%$) (Ref. 47) of a clean Ag(110)

surface may be attenuated with hydrogen concentration which, subsequently, could give rise to a change in the PES and bonding geometry, hence a shift in the vibrational energy.

Further possible indication of strong H-H interaction is inferred from the large energy dispersion of the hydrogen modes. At high coverages there exists a large energy dispersion, especially with scattering along the [001] direction. As can be seen in Fig. 5(a), with the scattering plane along the [001], the energy of the ~60-meV loss disperses downward by ~10 meV while the 104-meV loss disperses upwards (~5 meV). The top off-specular spectrum corresponds to a momentum transfer of $q_{\parallel} \cong 0.7$ Å^{-1} across the Brillouin zone ($\bar{\Gamma} \rightarrow \bar{Y}$:$q_{\parallel} = 0.77$ Å^{-1}). Similar dispersion behavior was observed for the H/Ni(110)-(2×1) hydrogen modes[35] and was also attributed to H-H interactions.

The work-function change ($\Delta\Phi$) as a function of hydrogen exposure is shown in Fig. 4(b). After steadily increasing with coverage, $\Delta\Phi$ maximizes at 0.22±0.02 eV at saturation. Assuming a charge transfer towards the proton ($H^{\delta+}$), the positive-energy shift supports the proposition that the majority of the hydrogen is adsorbed on the surface rather than being absorbed into the subsurface region, that is, the dynamic dipole lies outside the image charge plane. This proposition is in accordance with the EELS data and the hydrogen bonding site assignment.

D. Hydrogen desorption: TDS

Figure 7 shows a series of representative H_2 thermal-desorption spectra (TDS) as a function of coverage. The corresponding areas, $\int P_{H_2} dt$, are shown in Fig. 4(c). The TDS area versus the exposure curve agrees well with a simple Langmuir adsorption model, $\Theta(L) = \Theta_{sat}[1 - \exp(kL/\Theta_{sat})]$, which is also shown in Fig. 4(c). Because of the unknown efficiency of the atomic doser, the sticking rate constant k and corresponding initial sticking coefficient could not be determined. No evidence of atomic H desorption was observed in the exposure range or at the temperature ramp rate investigated.

Each TDS spectrum is characterized by two overlapping desorption curves with peak temperatures at ~155 (T_1^{peak}) and ~175 K (T_2^{peak}). These desorption temperatures are uncharacteristically low for most H/metal systems; for example, hydrogen desorbs from Cu(110) at ~325 K, Pd(110) at ~350 K, and Ni(110) at 250–350 K. The TDS spectra shown here are representative. That is, the exact shapes and area ratio between the two desorption peaks varied slightly depending on the experimental conditions, e.g., temperature ramp rate, slight sample contamination, and prior annealing temperature; however, the total integrated H_2 intensity remained approximately constant for identical initial coverages.

In order to extract the kinetic reaction orders n and the activation energies for desorption E_{des} of the two states, an analysis based on a modified Arrhenius plot[48] was utilized using a number of TDS spectra. Assuming desorption kinetics following the Polanyi-Wigner rate expression,[49]

$$\text{rate} = -\frac{d\Theta}{dt} = \nu_n \Theta(t)^n \exp\left[-\frac{E_{des}}{kT}\right], \tag{2}$$

a plot was constructed for each spectrum at a given initial coverage of the form $[\ln(-d\Theta/dt) - n\ln(\theta)]$ versus $(1/T)$, where $d\Theta/dt$ is proportional to the measured H_2 desorption rate, Θ is the adsorbate coverage, and ν is the preexponential factor. In Fig. 8, a representative plot of this type is shown corresponding to a saturation coverage of hydrogen. Note that over the desorption region of either peak, the modified Arrhenius plot is linear for only one specific value of n and the slope determines E_{des}. An analysis of ~20 TDS spectra independently yielded minimum chi-squared fitting values for $n = 1$ ($n = 2$) for the lower- (higher-) temperature desorption state. Fur-

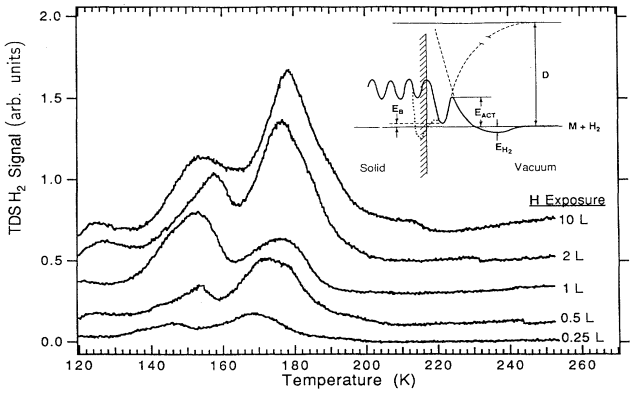

FIG. 7. Thermal-desorption spectra of H_2 from Ag(110) for a variety of initial H exposures at 100 K. The inset shows a representative potential-energy surface for the interaction of hydrogen with a simple- or noble-metal surface. (E_{H_2} = physisorption energy; E_{ACT} = activation energy; E_B = chemisorption energy; D = H_2 dissociation energy.)

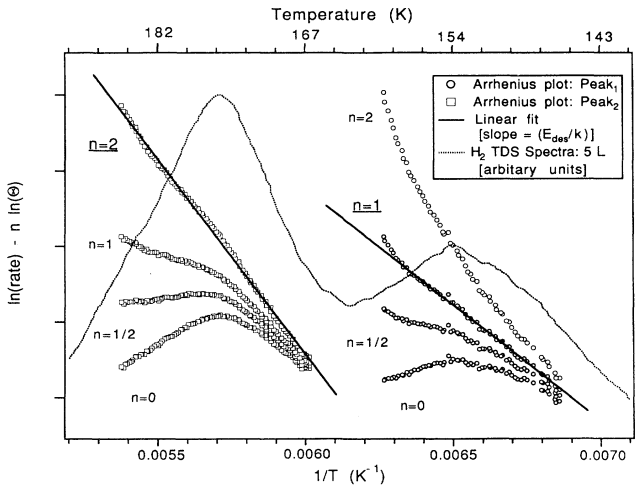

FIG. 8. Reaction order plot of H_2 desorption from Ag(110). The straight line is a least-squares fit through data points and the slope yields the desorption energy (dotted line: TDS data for the initial saturation H coverage.)

thermore, the average desorption energies were determined to be 0.30±0.035 eV (6.9±0.8 kcal/mol) for the $n=1$ state and 0.43±0.07 eV (9.95±1.6 kcal/mol) for the $n=2$ state. Because this analysis fails to account for any H-H interaction mechanism, these determined values are, at best, only an estimation; however, analogous to the low desorption temperatures, the determined $E_{\rm des}$'s are relatively small compared to most H/metal systems.

Compared to similar noble- and simple-metal systems such as Cu,[36] Al,[50] or Mg (Ref. 23) the H_2 desorption temperature of Ag(110) is quite low. It is known that this low hydrogen energy binding state is not limited to the (110) surface; the chemisorption characteristics of the H/Ag(111) system are quite similar.[48] At low coverage, the desorption from Ag(111) ($T^{\rm peak}\cong 170$ K) follows second-order kinetics with a desorption energy of 10 kcal/mol, a value which is almost identical to the ($T_2^{\rm peak}$) state of the Ag(110) system. Furthermore, evidence of second-order desorption of H_2 from Au(111) also yields a very low desorption energy (3 kcal/mol) with a $T^{\rm peak}$ of ~110 K.[51] If it is assumed that the H-metal bond is dominated by the overlap of the H(1*s*) orbital and the metal *sp* bands (*d* bands play a negligible role),[52] then H bonding with Ag and Au should be weaker than with Al, Cu, and Mg. That is, the fact that the bottom of the *sp* bands of Ag and Au are closer to E_F decreases the amount of overlap with the relatively higher binding energy of the H(1*s*) state and consequently the strength of the H-metal bond should be weaker.

The inset in Fig. 7 shows a representative PES for the interaction of hydrogen with the Ag(110) surface. Note that the energy barrier to desorption ($E_{\rm des}$) is the sum of the height of the activation barrier to dissociative adsorption ($E_{\rm act}$) and the adsorption site binding energy (E_B). Thus if we assume that $E_{\rm act}$ is $\gtrsim 0.5$ eV, as theory predicts, and measure a desorption energy less than 0.5 eV, the binding energy should be positive relative to the energy at large H_2-Ag surface separation.[53] This implies that this state is then thermodynamically unstable. However this one-dimensional PES description of the hydrogen-surface interaction may be too simplistic. Conflicting results from a series of experiments[16,18,54] which measured $E_{\rm act}$ for the H_2-Cu surface interaction may indicate that the desorption and adsorption PES's differ. It has been suggested that desorption characteristics may be dominated by small concentrations of surface defects.[55] Finally, the fact that each TDS spectrum of the H/Ag(110) system has two desorption peaks indicates a lack of a simple PES. Possible explanations for multiple peaks in TDS spectra are desorption from differing bonding sites (surface→surface transition), the effects of large H-H interactions, or the concomitant subsurface diffusion (overlayer→underlayer transition) and surface reconstruction during the desorption process.

E. Atomic hydrogen bonding and structure > 100 K: EELS and LEED

In an attempt to understand the "two-peak" phenomena of the TDS data, EELS and LEED data were collected as a function of partial annealing temperatures. That is, after adsorption of atomic hydrogen at 100 K, the crystal was annealed, at the same ramp rate as the TDS experiments, to a given temperature and then recooled. Figure 9 shows a comparison between the vibrational spectrum at ~100 K of the hydrogen saturated system and after a partial annealing cycle to ~165 K. Note that this temperature corresponds to the approximate minima between the two desorption peaks observed with TDS. The large differences in the vibrational spectra before and after annealing clearly indicate a new bonding geometry. Thus, the "two-peak" TDS phenomena can be explained in terms of desorption from a low-temperature bonding site coupled with a conversion to a new bonding site via thermal diffusion and/or accompanying surface reconstruction. That is, a fraction of the hydrogen desorbs and the remaining converts to a new phase of lower-energy configurations. Because the new bonding geometry configuration remains after recooling, this transformation is irreversible.

The EELS spectra show that intense loss located at ~60 meV at low temperature is absent in the higher-temperature activated phase. The new EELS spectrum is replaced by vibrational losses at ~72, 94, and 118 meV. Not only does the elastic peak drop by a factor of 2 after the transition (indicating an increased surface disorder), but the loss intensities relative to the elastic peak also decrease by a factor of 2. The FWHM's of the new losses, in general, also decrease. With the EELS scattering plane along both high-symmetry directions, the 94-meV loss is strongly dipole active, whereas the 72 and 118 meV are weakly dipole active. Because this phase is observed following a difficult annealing/desorption experimental sequence, the relative and absolute peak intensities, widths, and peak positions varied slightly from spectrum to spectrum.

This thermally induced change in bonding geometry is also accompanied by a change in the LEED pattern. Upon annealing to ~165 K and recooling, a dim (1×2)

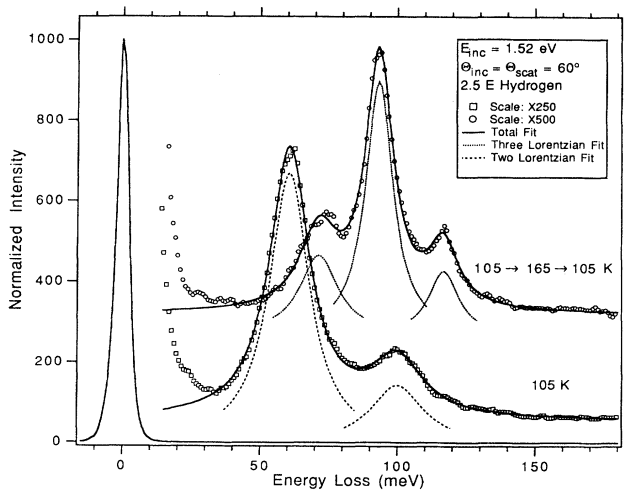

FIG. 9. Specular EELS spectra of low-temperature H/Ag(110) (bottom spectrum) and the same system after a partially annealing to 165 K (top spectrum). The solid line is the sum of fitted Lorentzian line shapes through the loss peaks.

structure and large increase in the diffuse background is observed with LEED. As in the low-temperature (2×2) phase, the half-order spots are elongated along the [001] direction. The rise in the diffuse background as well as an attenuation in the EELS elastic peak indicate a decrease in long-range order; that is, the surface is rougher. At coverages less than saturation, the intensity of the (1×2) "extra" LEED spots and diffuse background are proportionately dimmer.

In some aspects, this high-temperature phase transformation is similar to the H/Cu(110) system. The low-temperature phase of the H/Cu system also undergoes an irreversible transition at ~170 K in which a change in vibrational spectrum is accompanied by a (1×2) LEED pattern. Based on He diffraction data, Rieder and Stocker[55] suggested that the H/Cu-(1×2) LEED structure can be explained in terms of a subsurface reconstruction. However, other studies[32,36] have claimed that the (1×2) structure is due to a missing-row-type reconstruction based on EELS data. Although the "extra" LEED spots in the H/Cu system are relatively more intense and sharper than in the H/Ag system, the high-temperature EELS spectra between the two systems are remarkably similar; except for a linear energy scaling, the loss energies and relative intensities are almost identical. This may imply that if the bonding geometry is similar, then the dim (1×2) pattern of the H/Ag(110) system may also correspond to the proposed missing-row-type reconstruction.

The H/Ni(110) system also has a high-temperature phase. At saturation coverage, the low-temperature H/Ni-(1×2) row-pairing structure converts irreversibly to a "streaky" (ST) (1×2) hydrogen phase upon annealing to ~200 K. Although the structure of this phase has been debated in the past, a recent STM study[56] concludes that the structure of this high-temperature (ST) phase is a missing-row structure. Moreover, the reconstruction is caused by very local effects, the formation of -Ni-H- chains along the [1$\bar{1}$0] direction.

In order to better elucidate the structure of this high-temperature phase, LEED-*IV* profiles of five inequivalent integer-order spots (total-energy range ≥2 keV) were recorded from the clean Ag(110)-(1×1) surface, the H/-(1×2) phase, and also the K($\Theta_K \cong 0.1$ ML)/-(1×2) phase, which is known to be a missing-row-type reconstruction.[47] The experimental profiles of each system were then compared via an averaged mean-square difference technique.[57] The result of this somewhat cursory analysis suggests that the H/-(1×2) structure does not correspond to the long-range missing-row-type reconstruction induced by small amounts of adsorbed K. However, the combination of low intensity half-order spots, large diffuse background, and lack of a hydrogen saturation may indicate that the H/-(1×2) phase is due to the formation of small islands of a missing-row-type reconstruction wherein only short-range order exists. It is known that if this high-temperature phase is recooled and subsequently reexposed to additional atomic hydrogen, the EELS spectrum consists of both high- and low-temperature phase losses. This corroborates the suggestion that the high-temperature H/-(1×2) phase is limited to small islands. The LEED pattern after reexposure also reflects a mixture of these two temperature phases. Thus, similar to the H/Ni and possibly the H/Cu systems, an island missing-row model explains most of the qualitative observations of the high-temperature H/Ag(110) system.

If a missing-row model is assumed, the vibrational losses of the high-temperature EELS spectra are probably due in part to hydrogen occupying tilted-trigonal sites on the [111] microfacet. As previously alluded to, this assignment is in accordance with the high-temperature results of other H/fcc(110) systems. However, based on the number of EELS losses, the hydrogen is probably not limited to this single bonding site. The weaker intensities and narrower widths of the EELS losses in Fig. 9 suggest that hydrogen may occupy subsurface sites, wherein the dynamic dipole is more fully screened.

Hydrogen is known to occupy subsurface sites on a number of different metals. Based on atomic hydrogen implantation experiments, Baddorf *et al.* have suggested that the high-temperature EELS spectra of the H/Cu(110) system reflect hydrogen occupation of both surface tilted trigonal and subsurface tetrahedral sites, in approximately equal quantities.[36] If the hydrogen occupies subsurface sites, the dim (1×2) LEED pattern may be caused by a subsurface-type reconstruction. Preliminary NRA data of the D/Ag(110) system indicate an occupation of subsurface and/or bulk sites upon extremely high exposures of atomic deuterium.[58]

IV. DISCUSSION AND SUMMARY

We have found that the interaction of hydrogen with the surface of Ag(110) has many observable characteristics which are quite similar to that of other H/fcc(110) noble- and transition-metal systems. As in these similar H/metal systems, it has been shown that the interaction of hydrogen with the Ag(110) surface is definitely not "simple" as one might naively expect. The complexity includes the possibility of hydrogen absorption into subsurface/bulk sites, the formation of a low- and high-temperature chemisorption phases, and substrate structural reconstructions/relaxations.

It has been proposed[2,59] that the propensity for hydrogen-induced structural reconstruction is related to the bulk cohesive energies (E_{coh}) (Ref. 60) of the substrate. For example, within the group-VIII metals, no H-induced strong reconstruction is observed for Rh, Ir, and Pt ($E_{coh} \geq 5.75$ eV/atom), however, Co, Ni, and Pd (4.44 eV/atom $\geq E_{coh} \geq 3.89$ eV/atom) form (1×2) reconstructions. With the exception of Mn, Ag has the lowest cohesive energy ($E_{coh} = 2.95$ eV/atom) of any of the transition or other noble metals. If this general trend is correct, then silver should reconstruct under the influence of chemisorbed hydrogen. This supports the argument that the LEED patterns of the low- and high-temperature phases of H/Ag(110) are caused, in part, by varying degrees of substrate reconstruction (strong or weak).

As stated in the Introduction, one structural study, using He diffraction data, has been completed on the deuterium "asymptotic" coverage phase of the D/Ag(110)

system.[8] The investigation concludes that this phase is characterized by a $c(4\times4)$ structure which includes both normal rippling of the $[1\bar{1}0]$ rows and small perpendicular surface "wiggles" along the [001] direction. Because this was the only structure which was reproducibly separated and the preparation techniques differed from our methods, it is uncertain which phase this corresponds to in the study presented here. Nevertheless, our conclusion that hydrogen induces some degree of Ag surface reconstruction is in agreement with conclusions of this earlier study.

In summary, the following has been shown.

(i) Dissociative or associative chemisorption of H_2 on the Ag(110) surface is an activated process as in the case of other noble- and simple-metal surfaces.

(ii) At $\sim$100 K, the EELS spectra of chemisorbed atomic hydrogen is very similar to H/transition-metal surfaces which also have twofold symmetry. Like these systems, hydrogen is chemisorbed on the surface in tilted-trigonal sites. In this phase, the H-H interaction dictates the lattice-gas structure, which varies depending on the surface concentration of hydrogen. The LEED diffraction patterns reflect these ordered arrays ("zig-zag" chains) as well as a weak reconstruction which accompanies the chemisorption.

(iii) Desorption of H_2 is characterized by two low-energy (low-temperature) peaks which follow first- and second-order kinetics similar to Ag(111) and Au(111).

(iv) Not unlike other similar systems, recooling after annealing to $\sim$165 K allows the surface to undergo an irreversible transition to a lower-energy configuration (the low-temperature phase is metastable). Similar to other systems, it is suggested that the surface undergoes a hydrogen-induced missing-row-type reconstruction over small island areas.

ACKNOWLEDGMENTS

This work was supported by the National Science Foundation on Grant No. DMR-89-03306 and NEDO (New Energy and Industrial Technology Development Organization) of Japan.

*Present address: Institute of Physics and Astronomy, Aarhus University, DK-8000 Aarhus C, Denmark.

[1]K. Christmann, Surf. Sci. Rep. **9**, 1 (1988); Mol. Phys. **66**, 1 (1989), and references cited therein.

[2]K. Christmann, Z. Phys. Chem. **154**, 145 (1987), and references cited therein.

[3]W. Moritz and D. Wolf, Surf. Sci. **163**, L655 (1985).

[4]C. M. Chan and M. A. Van Hove, Surf. Sci. **171**, 226 (1986).

[5]M. Copel and T. Gustafsson, Phys. Rev. Lett. **57**, 723 (1986).

[6]P. Fery, W. Moritz, and D. Wolf, Phys. Rev. B **38**, 7275 (1988).

[7]C. L. Fu and K. M. Ho, Phys. Rev. Lett. **63**, 1617 (1989).

[8]P. Cantini, L. Mattera, M. F. M. De Kieviet, K. Jalink, C. Tassistro, S. Terreni, and U. Linke, Surf. Sci. **211/212**, 872 (1989).

[9]B. Reihl, R. R. Schlittler, and H. Neff, Surf. Sci. **152/153**, 231 (1985).

[10]Initial sticking coefficients for H_2 dissociative chemisorption on transition fcc(110) metals is typically near unity (Ref. 1).

[11]P. Nordlander, S. Holloway, and J. K. Nørskov, Surf. Sci. **136**, 59 (1984).

[12]R. Sporken, P. A. Thiry, F. F. Pireaux, and R. Caudano, Surf. Sci. **160**, 443 (1985).

[13]J. Harris, T. Rahman, and K. Yang, Surf. Sci. **198**, L312 (1988).

[14]J. Harris, Surf. Sci. **221**, 335 (1989).

[15]D. Halstead and Holloway, J. Chem. Phys. **93**, 2859 (1990).

[16]M. Balooch, M. J. Cardillo, D. R. Miller, and R. E. Stickney, Surf. Sci. **46**, 358 (1974).

[17]L. Stobiński and R. Duś, Surf. Sci. **269/270**, 383 (1992).

[18]G. Anger, A. Winkler, and K. D. Rendulic, Surf. Sci. **220** (1989).

[19]B. E. Hayden and C. L. Lamont, Phys. Rev. Lett. **63**, 1823 (1989).

[20]H. F. Berger and K. D. Rendulic, Surf. Sci. **253**, 325 (1991).

[21]J. Paul and F. M. Hoffmann, Surf. Sci. **194**, 419 (1988).

[22]K. B. Ray, J. B. Hannon, and E. W. Plummer, Chem. Phys. Lett. **171**, 469 (1990).

[23]P. T. Sprunger and E. W. Plummer, Chem. Phys. Lett. **187**, 559 (1991).

[24]P. T. Sprunger and E. W. Plummer, Surf. Sci. (to be published).

[25]D. P. Woodruff, G.-C. Wang, and T.-M. Lu, in *The Chemical Physics of Solid Surfaces and Heterogeneous Catalysis,* edited by D. A. King and D. P. Woodruff (Elsevier, New York, 1983), Vol. 3, p. 319.

[26]W. Puchta, W. Nichtl, W. Oed, N. Bickel, K. Heintz, and K. Müller, Phys. Rev. B **39**, 1020 (1989).

[27]LEED-*IV* of the diffraction spots (10), (01), (02), $(0,\frac{1}{3})$, and $(0,\frac{2}{3})$, $(1,\frac{1}{3})$ and $(1,\frac{2}{3})$, and $(0,\frac{4}{3})$ and $(0,\frac{5}{3})$ were used in the calculation.

[28]This simple calculation assumes that the surface Debye temperature corresponding to the fractional and integer spots is nearly equal.

[29]K. Christmann, R. J. Behm, G. Ertl, M. A. Van Hove, and W. H. Weinberg, J. Chem. Phys. **70**, 4168 (1979).

[30]K. Lehnberger, W. Nichtl-Pecher, W. Oed, K. Heinz, and K. Müller, Surf. Sci. **217**, 511 (1989).

[31]V. Penka, K. Christmann, and G. Ertl, Surf. Sci. **136**, 307 (1984).

[32]B. E. Hayden, D. Lackey, and J. Schott, Surf. Sci. **239**, 119 (1990).

[33]K. W. Jacobsen and J. K. Nørskov, Phys. Rev. Lett. **59**, 2764 (1987).

[34]M. J. Puska, R. M. Nieminen, M. Manninen, B. Chakraborty, S. Holloway, and J. M. Nørskov, Phys. Rev. Lett. **51**, 1081 (1983).

[35]B. Voigtländer, S. Lehwald, and H. Ibach, Surf. Sci. **208**, 113 (1989).

[36]A. P. Baddorf, Ph.D. disseration, University of Pennsylvania, 1987.

[37]M. Conrad, M. E. Kordesch, R. Scala, and W. Stenzel, J. Electron Spectrosc. Relat. Phenom. **38**, 289 (1986).
[38]M. J. Puska and R. M. Nieminen, Surf. Sci. **157**, 413 (1985).
[39]C. Astaldi, A. Bianco, S. Modesti, and E. Tosatti, Phys. Rev. Lett. **68**, 90 (1992).
[40]H. Ibach and D. L. Mills, *Electron Energy Loss Spectroscopy and Surface Vibrations* (Academic, New York, 1982).
[41]N. J. DiNardo and E. W. Plummer, Surf. Sci. **150**, 89 (1985).
[42]H. Conrad, W. Stenzel, and M. E. Kordesch (unpublished).
[43]D. Skottke, R. J. Behm, G. Ertl, V. Penka, and W. Moritz, J. Chem. Phys. **87**, 6191 (1987).
[44]T. H. Ellis and M. Morin, Surf. Sci. **216**, L351 (1989).
[45]A. P. Baddorf, I.-W. Lyo, E. W. Plummer, and H. L. Davis, J. Vac. Sci. Technol. A **5**, 782 (1987).
[46]Geunsop Lee, P. T. Sprunger, and E. W. Plummer, J. Vac. Sci. Technol. (to be published).
[47]J. W. M. Frenken, R. L. Krans, J. F. van der Veen, E. Holub-Krappe, and K. Horn, Phys. Rev. Lett. **59**, 2307 (1987).
[48]D. H. Parker, M. E. Jones, and B. E. Koel, Surf. Sci. **233**, 65 (1990), and references therein.
[49]D. A. King, Surf. Sci. **47**, 384 (1975).
[50]A. Winkler, G. Požgainer, and K. D. Rendulic, Surf. Sci. **251/252**, 886 (1991).
[51]B. D. Kay, K. R. Lykke, and S. J. Ward (unpublished).
[52]X.-L. Zhou, J. M. White, and B. E. Koel, Surf. Sci. **218**, 201 (1989).
[53]J. Harris, Appl. Phys. A **47**, 63 (1988).
[54]K. D. Rendulic, Appl. Phys. A **47**, 55 (1988).
[55]K. H. Reider and W. Stocker, Phys. Rev. Lett. **57**, 2548 (1986).
[56]L. P. Nielsen, F. Besenbacher, E. Lægsgaard, and I. Stensgaard, Phys. Rev. B **44**, 13 156 (1991).
[57]M. A. Van Hove, S. Y. Tong, M. H. Elconin, Surf. Sci. **64**, 85 (1977).
[58]P. T. Sprunger and E. W. Plummer (unpublished).
[59]D. Tománek and K. M. Bennemann, Surf. Sci. **163**, 503 (1985).
[60]Taken from C. Kittel, *Introduction to Solid State Physics* (Wiley, New York, 1986).

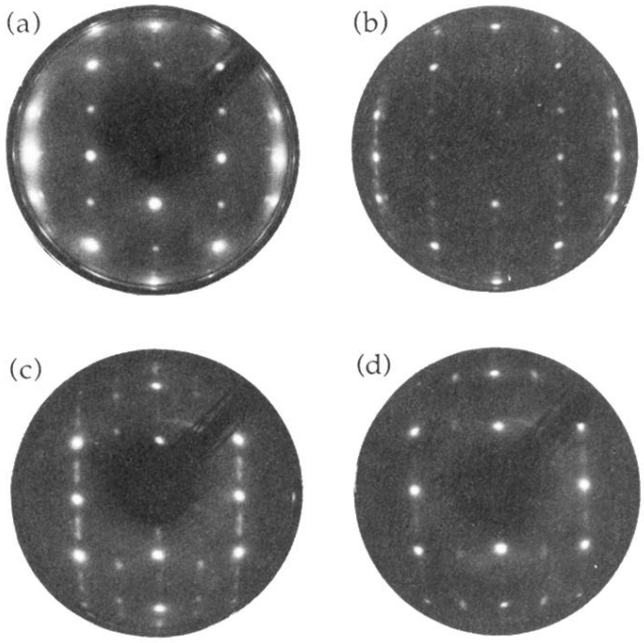

FIG. 1. The LEED pattern of (a) clean (1×1) (140 eV); (b) 0.7 L hydrogen (1×3) (140 eV); (c) 1 L hydrogen (2×6) (90 eV); and (d) 15 L hydrogen (2×3) (90 eV). Sample temperature = 100 K.